Trapped Field Profiles on Square GdBaCuO Bulks with Different Arrangement of Growth Sector Boundaries

2012 Jpn. J. Appl. Phys. 51 093005

(http://iopscience.iop.org/1347-4065/51/9R/093005)

Japanese Journal of Applied Physics 51 (2012) 093005 **REGULAR PAPER**
http://dx.doi.org/10.1143/JJAP.51.093005

Trapped Field Profiles on Square GdBaCuO Bulks with Different Arrangement of Growth Sector Boundaries

Hiroyuki Fujishiro[1]*, Takahiro Arayashiki[1], Takuya Tamura[1], Tomoyuki Naito[1], Hidekazu Teshima[2], and Mitsuru Morita[2]

[1]*Faculty of Engineering, Iwate University, Morioka 020-8551, Japan*
[2]*Advanced Technology Research Laboratories, Nippon Steel Corporation, Futtsu, Chiba 293-8511, Japan*

Received June 3, 2012; accepted June 25, 2012; published online August 28, 2012

Square GdBaCuO bulks with 45.2 x 45.2 mm^2 in the *ab*-plane and 15 mm in thickness along the *c*-axis with different arrangements of growth sector boundaries (GSBs) were magnetized by a field-cooled magnetization (FCM), a zero-field cooled magnetization (ZFC), and a pulsed-field magnetization (PFM) and the trapped field profiles were measured. For the lower applied field in ZFC, the magnetic flux was trapped in the growth sector regions (GSRs), independent of the arrangement of GSBs. For the lower applied field in PFM, the magnetic flux was mainly trapped in the GSRs and an additional flux was also trapped at the sides in both bulks because of the complicated flux intrusion by the local heat generation. These bulks can trap a magnetic field as high as 7.5 T at 50 K by FCM without destruction. The magnetic flux intrusion and trapping for the square bulks were discussed.

1. Introduction

REBaCuO superconducting bulks (RE: rare earth element and Y) are used as conductors with zero resistance for power current leads, as levitation devices using a pinning effect, and as high-strength bulk magnets using a strong pinning force.[1] To magnetize the bulk as a strong quasi-permanent magnet, field-cooled magnetization (FCM) using a superconducting coil magnet (SM) is a usual technique and can maximize the trapped field. Disk-shaped REBaCuO bulks are commonly used for basic study and practical applications. Many research groups have extensively investigated the trapped magnetic field behavior in bulk superconductors.[2–6] Square or rectangular bulks have also been fabricated and used for specific applications such as a flywheel,[7] magnetic bearings,[8] and a magnetic separation system.[9] We have developed a bulk magnet system with five-aligned square REBaCuO bulks, which has been used for magnetic separation to purify waste water.[10,11] The square bulk is grown from an identical-shaped precursor,[12] or is cut from a disk bulk.[13] The influences of the shape of the bulk and the arrangement of growth sector boundaries (GSBs) on the flux intrusion path, the trapped field profile, and the mechanical strength have not been investigated, compared with the disk bulk.

As magnetizing methods for the REBaCuO bulks other than FCM, there are zero-field cooled magnetization (ZFC) and pulsed-field magnetization (PFM). In the ZFC technique, the magnetic field is applied and decreased using SM on the cooled bulk lower than T_c, which is not a popular technique to magnetize the bulk because only half of the applied field can be trapped at the center of the disk bulk.[14] On the other hand, the PFM technique has been intensively studied because of the inexpensive and mobile experimental setup without the use of SM. Several approaches have been performed and have succeeded in enhancing the trapped field including by an iteratively magnetizing pulsed-field method with reducing amplitude (IMRA),[15] and a multi pulse technique with step-wise cooling (MPSC).[16] A two-stage PFM technique, named a modified MPSC (MMPSC), was proposed by us,[17] in which a record-high trapped field of 5.20 T was realized on the disk-shaped GdBaCuO bulk 45 mm in diameter at 30 K.[18] When the square bulk with different arrangements of GSBs is magnetized by PFM, different behaviors for the magnetic flux intrusion and the field trapping profile are supposed, compared with those for a disk-shaped bulk, because the distance of the flux intrusion path between the bulk periphery and the bulk center is not identical at each position in the square bulk.

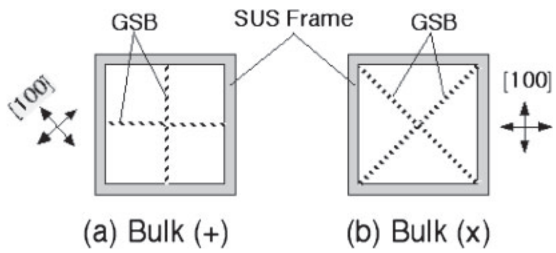

Fig. 1. Schematic view of two square-shaped bulks used in this study. In the Bulk(+), GSBs are positioned crosswise to the bulk, and in the Bulk(×), GSBs are positioned diagonally to the bulk.

In this study, we magnetized the square bulks with different arrangements of GSBs by FCM, ZFC, and PFM and compared the trapped field profiles. The flux intrusion and the flux trapping in the square bulk with different arrangements of GSBs are discussed.

2. Experimental Procedure

Two square-shaped GdBaCuO bulks (Nippon Steel) were used with an area of 45.2 × 45.2 mm^2 in the *ab*-plane and 15 mm in thickness along the *c*-axis, which were cut from a disk-shaped bulk 65 mm in diameter. The bulk crystals were composed of $GdBa_2Cu_3O_7$ (Gd123) and Gd_2BaCuO_5 (Gd211) with the molar ratio of Gd123 : Gd211 = 0.75 : 0.25, 10 wt% Ag_2O, and a small amount of Pt powder. Figure 1 shows a schematic view of the two square bulks used in this study, where the dotted lines showed the GSBs. In Fig. 1(a), GSBs are positioned crosswise to the bulk. Hereafter, we abbreviate this configuration as Bulk(+). In Fig. 1(b), GSBs are positioned diagonally to the bulk, where we abbreviate this configuration as Bulk(×). The bulks were tightly mounted in a stainless (SUS316L) frame 5 mm in thickness using a Stycast 2850GT resin.

*E-mail address: fujishiro@iwate-u.ac.jp

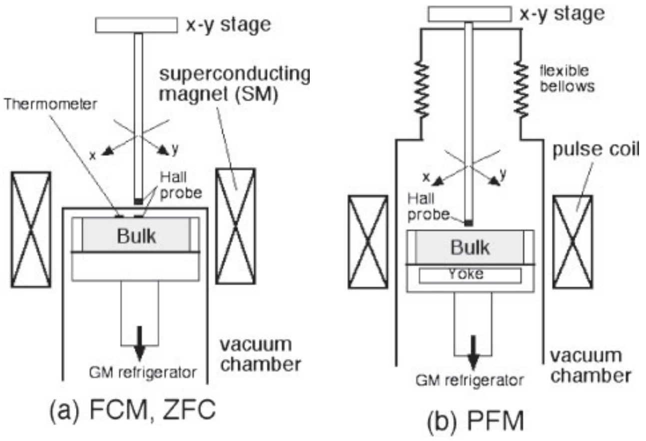

Fig. 2. Experimental setup for (a) FCM and ZFC and (b) PFM around the bulk and the magnetizing coil.

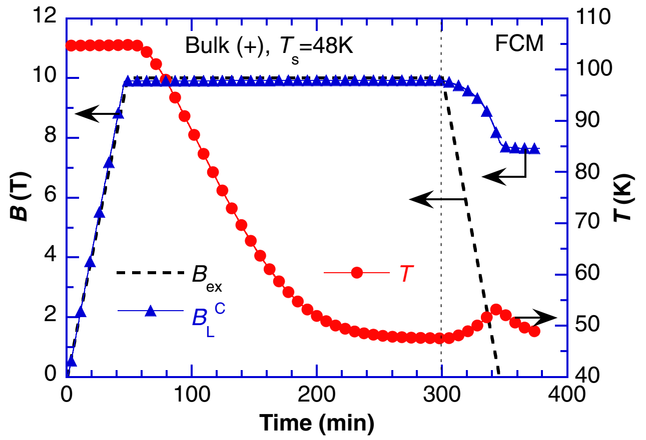

Fig. 3. (Color online) Time dependence of applied field $B_{ex}(t)$, local field $B_L{}^C(t)$, and temperature $T(t)$ on the Bulk(+) magnetized by FCM at 48 K.

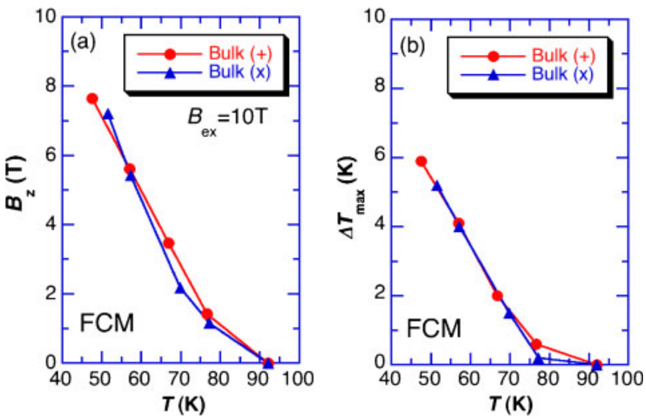

Fig. 4. (Color online) Temperature dependence of (a) trapped field B_z and (b) maximum temperature rise ΔT_{max} on the Bulk(+) and Bulk(×) magnetized by FCM.

Figure 2(a) shows the experimental setup for FCM and ZFC. The bulk was mounted tightly on the cold stage of a Gifford–McMahon (GM) cycle helium refrigerator. For FCM, the magnetic field of 10 T was reduced to zero at $-0.224\,\mathrm{T\,min^{-1}}$ at the temperature of the bulk, T_s = 48–80 K, using a cryo-cooled superconducting solenoid magnet (JASTEC JMTD-10T100). For ZFC, the magnetic field was increased at $0.224\,\mathrm{T\,min^{-1}}$ at $T_s = 77$ K, was kept at the maximum field of $B_{ex} = 1$ T for 15 min, and then reduced to 0 T at the same speed. Two-dimensional trapped field profiles, $B_z{}^{FCM}$(4 mm) and $B_z{}^{ZFC}$(4 mm), were measured on the vacuum sheath surface at a distance of $z = 4$ mm from the bulk surface, stepwise with a pitch of 1 mm by scanning an axial-type Hall sensor (F W Bell, BHA 921). The time dependences of the local magnetic fields $B_L{}^C(t)$ and temperatures $T(t)$ were measured, respectively, using the Hall sensor (F W Bell, BHT 921) and the Cernox thermometer, both of which were adhered on the center of the bulk surface.

Figure 2(b) presents the experimental setup for PFM. The bulk was tightly set on a soft iron yoke cylinder 60 mm in diameter and 20 mm in thickness and mounted similarly on the refrigerator. The magnetizing solenoid copper coil, which was cooled using liquid nitrogen, was placed outside the vacuum chamber. A single magnetic pulse B_{ex} with an amplitude from 2.5 to 6.4 T and with a rise time of 0.01 s and a duration of 0.1 s was applied to the bulk, which was cooled to $T_s = 40$ or 77 K. The trapped field profiles of $B_z{}^{PFM}$(1 mm) were mapped at a distance of $z = 1$ mm above the bulk surface, stepwise with a pitch of 1 mm by scanning the Hall sensor (BHA 921) inside the vacuum chamber using an x–y stage controller. We cannot measure the trapped field profiles for PFM and ZFC/FCM under an identical distance, z, from the top surface of the bulk because of the limitation of the experimental apparatus.

3. Results and Discussion

3.1 Field-cooled magnetization

Figure 3 shows examples of the time dependence of the applied field $B_{ex}(t)$, the local field $B_L{}^C(t)$ at the center of the bulk surface, and temperature $T(t)$ on the Bulk(+) at $T_s = 48$ K for FCM. During the descending stage for $t \geq$ 300 min, the temperature increased by about 6 K gradually and then recovered to the initial temperature. The local field $B_L{}^C(t)$ decreased from 10 T gradually, and finally, the magnetic field of $B_z = 7.65$ T was trapped on the center of the bulk surface.

Figures 4(a) and 4(b) present, respectively, the trapped field B_z and the maximum temperature rise ΔT_{max} for the Bulk(+) and Bulk(×) during FCM, as a function of T_s. The B_z and ΔT_{max} for each bulk increased monotonically with decreasing T_s and a small amount of the difference between two bulks can be detected, which may result from their performance differences such as local variation in J_c, critical temperature T_c, macrocracks or Ag particles, or some relationship with the GSB arrangement. However, note that the square GdBaCuO bulk with an area of 45.2 × 45.2 mm^2 can trap over 7.5 T at approximately 50 K without destruction, and B_z is independent of the arrangement of GSBs.

Figures 5(a) and 5(b) show the trapped field profiles $B_z{}^{FCM}$(4 mm) for the Bulk(+) at $T_s = 48$ K and Bulk(×) at $T_s = 52$ K magnetized by FCM. The trapped field profiles show the pyramidal profiles, which do not depend on the arrangement of GSBs. These results indicate that the

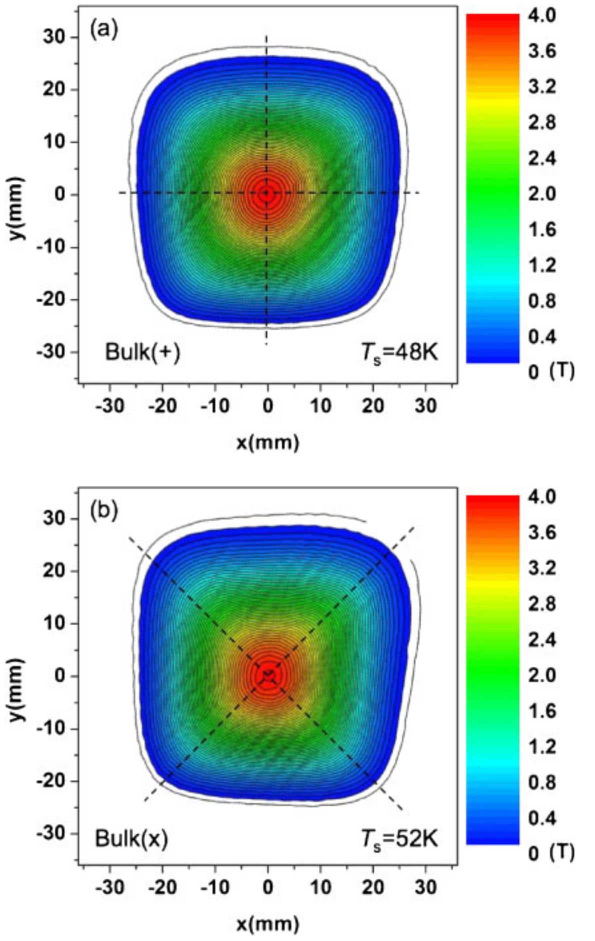

Fig. 5. (Color online) Trapped field profiles B_z^{FCM}(4 mm) on the square-shaped bulk of (a) Bulk(+) and (b) Bulk(×) magnetized by FCM.

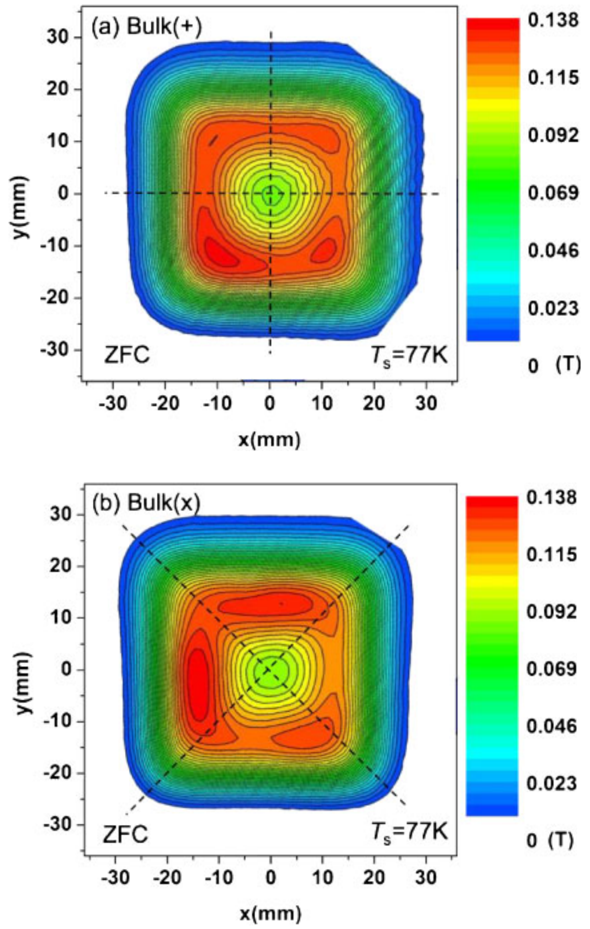

Fig. 6. (Color online) Trapped field profiles B_z^{ZFC}(4 mm) of (a) Bulk(+) and (b) Bulk(×) after the ZFC of $B_{\mathrm{ex}} = 1$ T at 77 K.

difference in the arrangement of GSBs cannot be detected by the trapped field profiles by FCM in the square bulk. However, in the disk bulk, trapped field profiles show conical profiles,[2–6] in which the arrangement of GSBs was detected by the trapped field profiles by FCM.

3.2 Zero-field cooled magnetization

Figures 6(a) and 6(b) present, respectively, the trapped field profiles B_z^{ZFC}(4 mm) for the Bulk(+) and the Bulk(×) at 77 K after the ZFC of $B_{\mathrm{ex}} = 1.0$ T. For an applied field as low as 1.0 T, where the magnetic flux can intrude only around the bulk periphery, a clear difference in the B_z^{ZFC}(4 mm) profiles can be seen between two bulks. In the profile of the Bulk(+) as shown in Fig. 6(a), the magnetic flux intruded and was trapped preferentially at the growth sector regions (GSRs), that is, at the corners of the square. GSRs mean the regions enclosed by GSBs. On the other hand, in the profile of the Bulk(×) as shown in Fig. 6(b), the magnetic flux was also trapped preferentially at the GSRs, that is, at the sides of the square. The critical current density J_c in GSRs is generally lower than that in GSBs and it is difficult for the flux to intrude and trap into the GSBs area for a lower B_{ex}.[19] Note that the trapped field profiles magnetized by ZFC are useful to confirm the J_c distribution (or the pinning force distribution) around the bulk periphery visually. In the experiment of ZFC, the temperature rise was as small as 0.1 K.

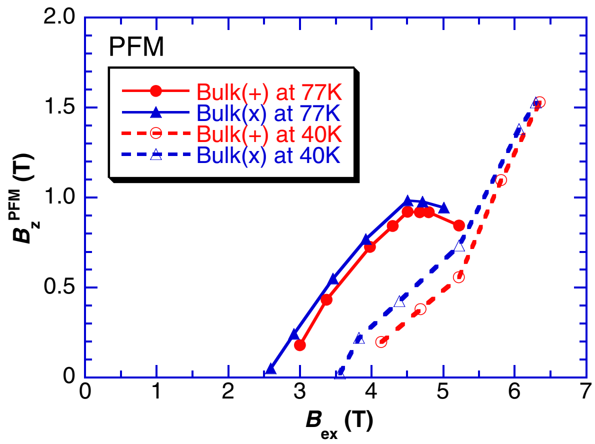

Fig. 7. (Color online) Trapped field B_z^{PFM}(1 mm) at the center of the bulk surface on the Bulk(+) and Bulk(×) as a function of applied pulsed field B_{ex} at 40 and 77 K.

3.3 Pulsed field magnetization

Figure 7 shows the trapped field B_z^{PFM}(1 mm) at the center of the bulk surface on the Bulk(+) and Bulk(×), as a function of applied pulsed field B_{ex} at 40 and 77 K. At $T_s = 77$ K, the magnetic flux starts to intrude and trap at $B_{\mathrm{ex}} =$ 2.5–3.0 T and B_z^{PFM}(1 mm) increases and takes a maximum at $B_{\mathrm{ex}} = 4.5$ T. At $T_s = 40$ K, the magnetic flux starts to

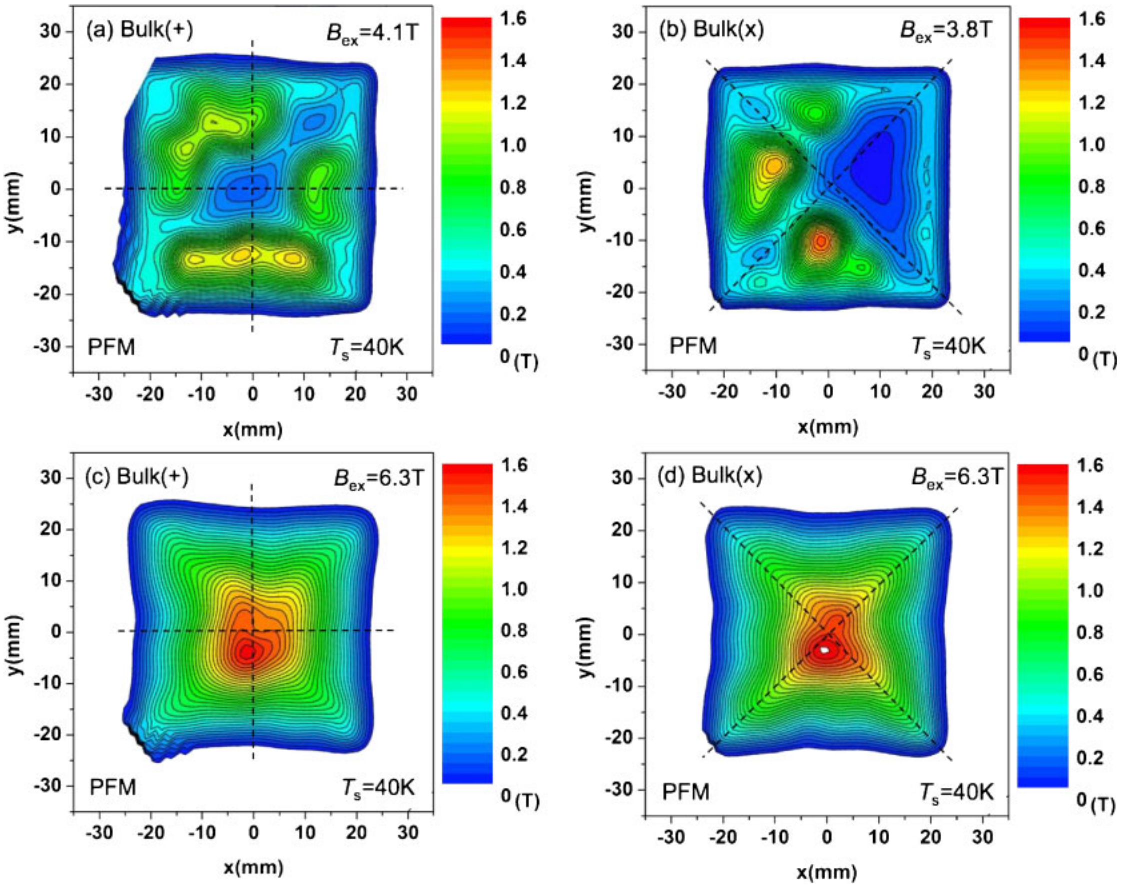

Fig. 8. (Color online) Trapped field profiles B_z^{PFM}(1 mm) of the Bulk(+) and Bulk(×) at $T_s = 40$ K for typical applied pulsed fields B_{ex}.

intrude and trap at 4 T and B_z^{PFM}(1 mm) increases monotonically with increasing B_{ex} up to 6.4 T. The shift of B_{ex}^0, at which the magnetic flux starts to intrude and trap, results from the increase in the J_c with decreasing temperature. These B_z^{PFM}(1 mm) vs B_{ex} characteristics are a common feature of PFM.[20] The difference in the characteristics between the Bulk(+) and Bulk(×) is very small, but the superconducting properties of the Bulk(+) seem to be slightly better than those of the Bulk(×).

Figure 8 shows the trapped field profiles B_z^{PFM}(1 mm) of the Bulk(+) and Bulk(×) at $T_s = 40$ K for typical applied pulsed fields B_{ex}. For a lower applied field around $B_{ex} = 4$ T, as shown in Figs. 8(a) and 8(b), the differences in the B_z^{PFM}(1 mm) profiles can be seen between two bulks. That is, in the Bulk(×) shown in Fig. 8(b), the magnetic flux was preferentially trapped at the GSRs except for the right GSR region. On the other hand, in the Bulk(+) shown in Fig. 8(a), the magnetic flux was also trapped at the sides of the bulk as well as that at the GSRs. These results do not always show consistency with those obtained by ZFC as shown in Fig. 6, although ZFC can be regarded as a kind of PFM technique in which the duration of the applied magnetic pulse is as long as 100–1000 s. The temperature rise during PFM is larger than that during ZFC owing to the fast motion of the magnetic flux.[21] Since the distance from the sides to the center is shorter than that from the corner to the center in the Bulk(+), it is easy for the magnetic flux to penetrate from the sides of the square bulk, even though the GSRs with lower J_c are positioned diagonally in the bulk. The difference in the length of GSBs may explain these phenomena. For a higher applied field of $B_{ex} = 6.3$ T, as shown in Figs. 8(c) and 8(d), the differences in the B_z^{PFM}(1 mm) profiles are small between two bulks. However, strictly speaking, the magnetic flux seems to be trapped preferentially on the GSBs in the Bulk(×).

4. Conclusion

We magnetized square GdBaCuO bulks with an area of 45.2×45.2 mm^2 in the *ab*-plane and 15 mm in thickness along the *c*-axis with different arrangements of GSBs by a FCM, a ZFC, and a PFM and measured the trapped field profiles. A summary of important results and conclusions obtained in this study is presented below.

(1) These bulks can trap the magnetic field over 7.5 T at 50 K by FCM without destruction. The trapped field profiles are pyramidal and the difference in the arrangement of GSBs cannot be detected using the profiles obtained by FCM.

(2) For the lower applied field for ZFC, the magnetic flux was mainly trapped in the GSRs, independent of the arrangement of GSBs in the square bulk. The trapped field profiles magnetized by ZFC are useful to confirm the J_c distribution or local variations in T_c (Gd/Ba solid solution) or microcracks or Ag particles around the bulk periphery visually.

(3) For the lower applied field for PFM, the magnetic flux was mainly trapped in the GSRs for both arrangements of GSBs and additional flux was also trapped at the sides in both bulks because of the complicated flux intrusion caused by the local heat generation.

Acknowledgment

This work is supported in part by a Grant-in-Aid for Scientific Research (No. 23560002) from the Ministry of Education, Culture, Sports, Science and Technology, Japan.

1) M. Murakami: Int. J. Appl. Ceram. Technol. **4** (2007) 225.
2) P. Gornert, P. Diko, W. Gawalek, T. Habisreuther, A. Kohler, D. Litzkendorf, T. Strasser, M. Wu, G. Krabbes, W. Bieger, P. Schatzle, G. Stoever, and U. Wiesner: *Advances in Superconductivity VIII* (Springer, Tokyo, 1996) 663.
3) G. Krabbes, G. Fuchs, P. Verges, P. Diko, G. Stoever, and S. Gruss: Physica C **378–381** (2002) 636.
4) R. Gonzalez-Arrabal, M. Eisterer, H. W. Weber, G. Fuchs, P. Verges, G. Krabbes, M. Tomita, M. Murakami, D. Litzkendorf, T. Habisreuther, and W. Gawalek: IEEE Trans. Appl. Supercond. **13** (2003) 3125.
5) D. A. Cardwell, Y.-H. Shi, N. Hari Babu, S. K. Pathak, A. R. Dennis, and K. Iida: Supercond. Sci. Technol. **23** (2010) 034008.
6) K. Xu, K. Tsuzuki, S. Hara, D. Zhou, Y. Zhang, M. Murakami, D. Nishio-Hamane, and M. Izumi: Supercond. Sci. Technol. **24** (2011) 085001.
7) J. Hull: Spectrum **34** (1997) 20.
8) J. R. Hull, M. Mulcahy, and J. F. Labataille: Appl. Phys. Lett. **70** (1997) 655.
9) H. Hayashi, K. Tsutsumi, N. Saho, N. Nishijima, and K. Asano: Physica C **392–396** (2003) 745.
10) T. Hiyama, H. Fujishiro, T. Tateiwa, T. Naito, H. Hayashi, and K. Tone: Physica C **468** (2008) 1469.
11) H. Fujishiro, T. Miura, T. Naito, and H. Hayashi: J. Phys.: Conf. Ser. **234** (2010) 032015.
12) M. Muralidhar, M. Tomita, K. Suzuki, M. Jirsa, Y. Fukumoto, and A. Ishihara: Supercond. Sci. Technol. **23** (2010) 045033.
13) H. Kamijo, T. Higuchi, H. Fujimoto, H. Ichikawa, and T. Ishigohka: IEEE Trans. Appl. Supercond. **9** (1999) 976.
14) T. Oka, K. Yokoyama, H. Fujishiro, and K. Noto: Supercond. Sci. Technol. **22** (2009) 065014.
15) Y. Yanagi, Y. Itoh, M. Yoshikawa, T. Oka, T. Hosokawa, H. Ishihara, H. Ikuta, and U. Mizutani: *Advances in Superconductivity XII* (Springer, Tokyo, 2000) 470.
16) M. Sander, U. Sutter, R. Koch, and M. Klaser: Supercond. Sci. Technol. **13** (2000) 841.
17) H. Fujishiro, M. Kaneyama, T. Tateiwa, and T. Oka: Jpn. J. Appl. Phys. **44** (2005) L1221.
18) H. Fujishiro, T. Tateiwa, A. Fujiwara, T. Oka, and H. Hayashi: Physica C **445–448** (2006) 334.
19) Y. Yanagi, Y. Itoh, T. Oka, H. Ikuta, and U. Mizutani: Supercond. Sci. Technol. **18** (2005) 839.
20) H. Fujishiro, T. Hiyama, T. Miura, T. Naito, S. Nariki, N. Sakai, and I. Hirabayashi: IEEE Trans. Appl. Supercond. **19** (2009) 3545.
21) H. Fujishiro, K. Yokoyama, T. Oka, and K. Noto: Supercond. Sci. Technol. **17** (2004) 51.

